Geochemical observations and one layer mantle convection

Nicolas Coltice and Yanick Ricard

N. Coltice and Y. Ricard, Laboratoire de Sciences de la Terre, Ecole Normale Supérieure de Lyon, 46 allée d'Italie 69364 Lyon cedex 07, France. (email: ncoltice@ens-lyon.fr; ricard@ens-lyon.fr)

Abstract

Rare gas systematics are at the heart of the discrepancy between geophysical and geochemical models. Since more and more robust evidence of whole mantle convection comes from seismic tomography and geoid modeling, the interpretation of high $^3He/^4He$ in some oceanic island basalts as being primitive has to be revisited. A time dependent model with 5 reservoirs (bulk mantle, continental crust, atmosphere, residual deep mantle and D") is studied for Rb/Sr and U/Pb/He systems. The dynamics of this model correspond to whole mantle convection in which subducted oceanic crust, transformed into dense assemblages, partially segregates to form a D" layer growing with time as in Christensen and Hofmann [1]. A complementary cold and depleted harzburgitic lithosphere remains above D". We assume that hotspots arise from the deep thermal boundary layer and tap, in variable proportions, material from both the residual deep mantle and D". The difference between HIMU and Hawaiian basalts is attributed to HIMU being mostly from strongly degassed oceanic crust, though enriched in incompatibles (D"), while Hawaii is mostly from MORB-source residuals that are variably degassed and depleted. We suggest that a significant part of the Earth's radioactive elements ($\sim$1/3) is trapped in the D" layer.

Key words: Mantle convection; isotopes; noble gases; mantle structure; box model.

1 Introduction

Current views of mantle stratification derived from geochemistry are often in contradiction with most recent geophysical observations. The former generally assumes the existence of independent reservoirs, including a pristine or more or less primitive lower mantle [2,3]. On the contrary, seismological imaging, interpretation of the large scale gravity field, and numerical simulation, all suggest a significant material exchange throughout the entire mantle [4–6].

It thus seems necessary to re-examine the geochemical observations on mantle stratification to see whether or not they can be interpreted in terms of large mass exchange in the whole mantle following the attempt by Albarède [7].

Rare gas systematics are at the heart of the contradiction between geochemistry and geophysics. Oceanic basalts often show contamination from atmospheric Xe, Ne and Ar. Therefore, we will focus on the interpretation of He that should be easier as He simply escapes from the mantle before being lost in space (although some reincorporation has been suggested [8]). The ^{4}He is the radioactive daughter of U or Th. Mantle rocks also contain the primordial isotope ^{3}He. During melting, the concentrations of an element in the melt C_{melt} and in the source C_{source} are related by a fractionation coefficient K

$$C_{melt} = K\,(F, D)\,C_{source} \tag{1}$$

This coefficient is related to the melt fraction F and to the partition coefficient between the solid and the melt, D

$$C_{solid} = DC_{melt} \tag{2}$$

Although various assumptions can be made to derive K, in the simplest case of batch melting one has

$$K = \frac{1}{F + D(1 - F)} \tag{3}$$

For two isotopes, D is the same and therefore isotopic ratios are conserved during melting. Isotopic measurements from mid ocean ridge basalts (MORBs) give ^{3}He/^{4}He=1.2 10^{-5} with very little dispersion [9]. Oceanic island basalts (OIBs) show much larger scattering from 0.7 10^{-5} at Mangaia [10] to 5 10^{-5} for the Loihi seamount [11,12].

Changes in the ^{3}He/^{4}He ratio should be reflected by changes in the ^{3}He/U ratio as U decay produces ^{4}He [13]. A high ^{3}He/^{4}He ratio means either a high content in ^{3}He or a low content in ^{4}He. The first hypothesis is commonly accepted: Loihi and Iceland hotspots are tapping a primitive and undegassed source while the MORB source is depleted and degassed (see references in [14]). The second hypothesis means that the source of high ^{3}He/^{4}He ratio is depleted in U and Th. This point of view has been shared by Anderson [8] and Albarède [7], although with different implications.

The degassed or undegassed nature of the source of hotspots should be determined by the direct observation of He abundances. However, these observations are much more ambiguous than isotopic ratios as the amount of escaped

gases at the surface is very difficult to estimate. The trace element concentrations of basalts can give information about the depletion of their source. As seen in Fig. 1, $^3He/^4He$ of some OIBs is anti-correlated with the U content; the more U depleted the basalt, the higher the $^3He/^4He$. As U is highly incompatible ($D = 0.005$), its fractionation during melting decreases with the melt fraction. When corrected for magma fractionation, the sources of Hawaiian basalts and MORBs have the same U content of 0.008 ppm [15]. This contradicts the interpretation of a primitive origin for the source of high $^3He/^4He$ basalts.

Isotopes other than rare gases have been used to infer mantle dynamics and imply that the OIB source is heterogeneous and made by a mixture between different end-members (see [14,16] for reviews). One of these end-members, called HIMU (high μ means high U/Pb), clearly shows recycling of oceanic crust. The HIMU source is explained by a process that fractionates U with respect to Pb. Such a U enrichment occurs in the oceanic crust by alteration and by dehydration during subduction. Even Hawaii shows evidence of crustal recycling, suggested by O [17], Os and Hf isotopes [18], even though its He ratio is described as primitive. The observed isotopic values (Pb, Os, Hf) require a long isolation period between 1 and 3 Ga.

2 Radioactive Sources

In addition to producing rare gases, U, Th and K are the sources of radioactive heat. It is well known that the budget of radioactive elements in the bulk silicate earth (BSE) cannot be balanced by the content of the continental crust (CC) and that of the MORB source extended to the whole mantle. A hidden reservoir of trace elements must exist (unsampled or poorly sampled). The balance of radioactive heat production rate for the BSE can be written:

$$H_{BSE} = H_{MORB\ source} + H_{CC} + H_{hid} \tag{4}$$

From the concentrations of U, Th and K in BSE and CC [19,20], the total heat production rate, H_{BSE}, is 19.9 TW, and H_{CC} is 10 TW, so that only 50% of the global radioactive heat is produced within the mantle. If the hidden reservoir corresponds to the lower mantle, its heat production rate is between 8.2 and 9.3 TW, leaving only 0.6 to 1.7 TW for the upper mantle (taking for the upper mantle, Th/U=2.5, K/U=12000 and $0.003 < C^U_{MORB\ source} < 0.008$ ppm). Notice that such a lower mantle cannot be primitive as a primitive lower mantle should have a heat production rate of 15 TW. If D" is the hidden reservoir with a thickness of 200 km, whereas the rest of the mantle is homogeneous with MORB-source composition, the D" heat production rate should be be-

tween 3.5 and 7.5 TW leaving 2.4 to 6.4 TW for the remaining bulk mantle. In this case the U content of D" would be between 0.08 and 0.18 ppm suggesting that it could be made of segregated oceanic crust as proposed by Hofmann and White [21].

The heat loss at the surface of the Earth is estimated to be 44.2 TW [22] from which we can subtract the crustal production to get a mantle heat loss of 34.2 TW. This includes a mantle production rate of 9.9 TW and a cooling contribution from mantle and core of 24.3 TW. The heat lost on top of the deep reservoir includes a radioactive contribution plus a cooling contribution (from this reservoir and from the core). This heat is transported to the surface by plume instabilities that give rise to hotspots at the Earth's surface. There are various indications that this heat has only a minor contribution to the total budget. From the oceanic swells, it is estimated to be as low as 2 TW [6,23] but this value is a lower limit and depends on the number of presumed hotspots. Convection modelers often consider that the bottom boundary layer is responsible for about 9 TW of the mantle heat flow (25 % of the mantle heat loss) [24].

If the hidden reservoir is the convective lower mantle, the heat loss at its top Q is proportional to its Rayleigh number Ra, $Q \sim Ra^{\beta}$ where β is of order 1/4-1/3. With commonly accepted thermal parameters, the Rayleigh number of the lower mantle is larger than that of the upper mantle and therefore most of the heat released at the surface should come from hotspots rising from 670 km depth. This is in contradiction with the observed low heat carried by hotspots. If the hidden reservoir is restricted to D", its small thickness would imply a very small Rayleigh number and thus a heat transport efficiency close to that of conduction. This would correspond to a heat loss already estimated between 3.5 and 7.5 TW associated with a temperature jump between 510 K and 1100 K. These values, especially the lower, are acceptable even when increased by a contribution from the core currently estimated around 3 TW [25]. A conductive D" reservoir could satisfy both geochemical and thermal considerations. It would bring to the bottom of the bulk mantle a total heat (radioactive production plus core cooling) amounting to 20% to 30% of the mantle heat loss. This layer should be denser than the "normal" lower mantle so as not to be swept off by convection, as discussed in the following.

3 Mantle convection

A number of geophysical results have made the hypothesis of a stratified model (at least stratified at 670 km depth) difficult to sustain. The most visual evidence comes from seismic tomography. Since Grand [26] we know that the Pacific subduction below North America is continuous through the whole mantle.

A similar pattern of downgoing slabs is observed below the Tethyan suture, from the Mediterranean sea to North of Australia [4,27,28]. On a larger scale, these models together with spherical harmonic models [29] indicate that the pattern of anomalies in the lower mantle corresponds closely to that of Mesozoic subductions.

The studies of the large scale geoid (the Earth's gravity equipotential) that is mostly perturbed by lower mantle mass anomalies also favor slab penetrations into the lower mantle. An easy and accurate way to explain the observed gravity is indeed to assume that slabs sink slowly in the lower mantle and that the present-day density anomalies are those associated with Mesozoic and Cenozoic subductions [5].

From a convection point of view, the stratification of the mantle could be produced by a density increase, a viscosity increase or by an effect due to endothermic phase transitions [30]. Although a composition difference is sometimes advocated, most of the velocity and density jumps across the transition zone can be explained by isochemical phase transformations [31]. The change with depth of the viscosity by 1-2 orders of magnitude [5] is not large enough to forbid a large mass exchange [6]. The commonly accepted values for the thermal expansivity and the Clapeyron slope of the spinel/perovskite + magnesiowustite transition do not prevent slab penetration into the lower mantle, directly or after some delay [24,32], and the mass exchanges in the long run are not different from a continuous mass flow [33].

Together with the viscosity increase, the decrease of the thermal expansivity, from $\sim 4\ 10^{-5}\ K^{-1}$ in the upper mantle to $\sim 10^{-5}\ K^{-1}$ near the CMB [34], makes the lower mantle rather sluggish. A final characteristic reinforces this relative low efficiency of deep mantle convection. The mantle is mostly heated from within rather than from below which means that the upward return flow is broad and slow, and quite stably stratified.

The bottom heat flow, coming out from the core or as we speculate, partially from D" is carried out by plume instabilities. The rising instabilities from a boundary layer are carrying the very material of their source [35]. Large entrainment of the surrounding mantle in plume heads has been invoked but does not likely occur for Earth-like convection regimes [36]. In addition to carrying the source material, hotspots also carry their temperature excess. The fact that hotspots seem only $\sim$ 200 K hotter than the adiabat while a temperature jump in excess of 1000 K should be associated with the CMB, has been taken as an indication that hotspots rise from a chemically stable layer [37].

4 Mantle mixing

Since McKenzie [38], many papers have studied the mixing properties of passive [39–41] and active tracers [1,42] in mantle convection. However, no general consensus emerges. By varying by only a small amount the characteristics of the convection, very efficient to highly inefficient mixing properties can be obtained [40]. In a rather smooth 3D flow field, totally unmixed islands can survive within a well mixed background [41]. At 3D, convection models seem to predict much slower mixing rates than what was deduced from 2D modeling [43].

The increase with depth of the mantle viscosity does not imply a strong difference in the mixing properties of the upper and lower mantle, i.e., in the sizes and elongations of heterogeneities. Well mixed zones of the upper mantle are introduced into the lower mantle while poorly mixed lumps from the lower mantle reach the surface. This process homogenizes the mixing of the whole mantle [44]. Convection modeling also predicts that the lower mantle with its low deformation rates stores the freshly subducted slabs. Although old and young anomalies can survive in it, the lower mantle is as depleted [33] and can be on average even younger than the upper mantle [44].

To satisfy the geochemical constraints on rare gases, a stratification in the residence times must exist. To modify the ^{3}He/^{4}He ratio significantly, a residence time of $\sim$1 byr is needed, comparable to the half-life of the parent element ^{238}U. To quantify the depth dependence of the residence time in whole mantle circulation, we perform a simulation of time-dependent 2D convection at high Rayleigh number, 10^7, in a Cartesian box of aspect ratio 6, using the software ConMan [45]. We assume that the mantle is mostly heated from within (20% from below) and that the viscosity increases by a factor 100 at 4/5 of the box thickness. At each depth z, the root mean square average (horizontally and in time) of the vertical velocity $\bar{v}(z)$ is computed. The residence time in each layer of thickness Δz is

$$T = \frac{2\Delta z}{\bar{v}(z) + \bar{v}(z + \Delta z)}. \tag{5}$$

The results of this calculation, depicted in Fig. 2, show that the bottom thermal boundary layer has a residence time much larger than the other layers and close to 1 byr. The explanation is that the boundary layer flow is dominated by horizontal kinematics caused by the pressure gradient between upwellings and downwellings. The cold downwellings need a very long time to re-heat and rise again. In fact the residence times are smallest ($\sim$50 myr) near the viscosity jump where the mass exchange is very large.

The D" layer could be a candidate for an isolated reservoir. It is associated with a density increase estimated from 25 kg.m^{-3} [46] to 70 kg.m^{-3} [47]. The density jump has a sign opposite to what would normally correspond to a hot lower boundary layer and is large compared to what can be obtained from thermal variations. With α=10^{-5} K^{-1} [34], a 50 kg.m^{-3} denser layer near the CMB should corresponds to a 1000 K colder zone. The density increase in D" could therefore be associated with a chemical rather than a thermal heterogeneity [48]. A possible explanation of D" properties can be derived from geodynamic modeling [1] and fluid dynamic experiments [49]: an excess density of the oceanic crust by a few percent (see [50–52]) with respect to the surrounding mantle could lead to the formation of a gravitationally stable layer by crustal segregation. Separation may occur when the slab rests close to the CMB or during a delamination near 670 km depth.

5 A box model of mantle chemistry

In the previous sections we have discussed various geochemical and geophysical constraints. We want now to show that all these observations are in agreement with a model in which a large mass flux exists throughout the transition zone. Although ultimately chemical exchanges will have to be modeled along with thermo-chemical convection models, this goal is presently out of reach: the convection codes are not able to generate plates self-consistently and to model oceanic and continental crust extraction. We are thus using a box model representation familiar to geochemists.

To describe the equations used in modeling the chemical transfer in the Earth with box models, we use the same formalism as in Albarède [7]. The mass M_i of a box i can be modified by output fluxes $Q_{i\to j}$ to j different boxes or by in-fluxes $Q_{j\to i}$ from these j boxes so that

$$\frac{dM_i}{dt} = \sum^{j\neq i} Q_{j\to i} - \sum^{j\neq i} Q_{i\to j} \tag{6}$$

We call C_i^k the concentration of the element k in the box i. The element k can be produced by the parent $k-1$ and produces the daughter element $k+1$. When a mass flux occurs between boxes i and j, the concentration of the element k can be enriched by a fractionation coefficient $K_{i\to j}^k$. The concentration C_i^k of the element k in the box i can vary by (a) radioactive decay, (b) output fluxes, (c) dilution, (d) input fluxes and (e) production from parent elements. This balance is expressed by

$$\frac{dC_i^k}{dt} = -(\lambda^k + \frac{\sum^{j\neq i} Q_{i\to j} K_{i\to j}^k}{M_i} + \frac{\sum^{j\neq i}(Q_{j\to i} - Q_{i\to j})}{M_i})C_i^k$$
$$+\frac{\sum^{j\neq i} Q_{j\to i} K_{j\to i}^k}{M_i} C_j^k + \lambda^{k-1} C_i^{k-1} \quad (7)$$

We consider a box model evolution of the Earth that includes 3 isotopic systems that seem to be independent: He related to degassing, Pb to recycling of oceanic crust and Sr to crustal extraction. These systems include the stable isotopes ^{3}He, ^{204}Pb ^{86}Sr, the radioactive parents ^{238}U, ^{235}U, ^{87}Rb and their associated daughters ^{4}He, ^{206}Pb, ^{207}Pb, ^{87}Sr.

5.1 Forward model

5.1.1 Reservoirs

The choice of two geochemical reservoirs is obvious: the continental crust (CC) and the atmosphere (AT). Geochemical differences between MORBs and OIBs provide strong evidence of the existence for at least three other reservoirs in the mantle. As advocated, one is chosen to be D". As the top of this layer is not well defined by seismology, its thickness is taken from 50 to 500 km.

The size of the high ^{3}He/^{4}He reservoir, referred to as the residual deep mantle (RDM), is at most that of the lower mantle. At least, its size can be reduced to that of the bottom boundary layer, estimated to be a few 100 km [53]. Therefore, we assume that the top of the high ^{3}He/^{4}He RDM, is located between 670 km depth and 100 km above the top of the D" layer. The last reservoir is the remaining bulk mantle (BM). A schematic diagram of our box model is given in Fig. 3. Table 1 gives the present-day masses of these various reservoirs. Notice that the oceanic crust and the associated harzburgitic lithosphere at the surface are complementary and included in the bulk mantle.

For simplicity we assume constant mass fluxes. Therefore the mass of each reservoir varies linearly with time (CC, D" and BM) or remains constant (RDM). The mass of CC divided by the age of the Earth represents the total flux from BM to CC, $Q_{BM\to CC} - Q_{CC\to BM} = M_{CC}/4.5\ Ga$. Similarly, as D" is also extracted from BM, $Q_{BM\to D"} - Q_{D"\to BM} = M_{D"}/4.5\ Ga$. This indicates that $Q_{BM\to CC}$ >6.5 10^{18} kg myr^{-1} and $Q_{BM\to D"} > 50\ 10^{18}$ kg myr^{-1} (assuming $M_{D"}$=200 10^{21}kg).

The present-day rate of crustal formation from back-arc tectonics is only around 2 10^{18} kg myr^{-1} [54]. As we think that D" consists of altered oceanic crust, $Q_{BM\to D"}$ should be comparable to the rate of oceanic crust production which is at present 60 10^{18} kg myr^{-1}. The rates of oceanic and continental

crust formation were certainly larger in the past [55] and we choose $Q_{BM\rightarrow CC}$ between 6 10^{18} and 12 10^{18} kg myr^{-1} and $Q_{BM\rightarrow D"}$ =180 10^{18} kg myr^{-1}.

We consider that RDM mass is at steady-state and thus, $Q_{BM\rightarrow RDM} = Q_{RDM\rightarrow BM}$. The buoyancy flux of plumes is estimated from the study of hotspot swells to be 1.73 10^{18} kg myr^{-1} [6,23]. The mass flux is obtained by dividing the buoyancy flux by $\alpha\Delta T$ where α is the thermal expansion coefficient (4 10^{-5} K^{-1}) and ΔT the excess temperature (250 K). This gives $Q_{RDM\rightarrow BM} = 170\ 10^{18}$ kg myr^{-1}.

The mass flux from BM to AT is negligible in Eq. 6, $Q_{BM\rightarrow AT} = 0$, but the helium flux is not, $Q_{BM\rightarrow AT}K^{He}_{BM\rightarrow AT}C^{He}_{BM} \neq 0$. The main outgassing process occurs at mid oceanic ridges, during oceanic crust (OC) extraction. Hence $Q_{BM\rightarrow AT}K^{He}_{BM\rightarrow AT}$ is taken to be $Q_{BM\rightarrow OC}K^{He}_{BM\rightarrow OC}$ with $Q_{BM\rightarrow OC} \sim Q_{BM\rightarrow D"}$ =180 10^{18} kg myr^{-1}. The coefficient $K^{He}_{BM\rightarrow AT}$ characterizes the fractionation of He between solid and melt before degassing.

Mass fluxes from AT or from CC to the deep mantle reservoirs (RDM or D") have been considered as negligible. We also consider that a hypothetical gravitationally stable D" does not exchange with RDM. The mass flux from the deep layers RDM and D" to CC should not be zero as some hotspots are reaching the continents possibly forming exotic terrains. From the volumes of the observed flood basalts on continents, we estimate that this mass flux is lower than 10^{18} kg myr^{-1}, an order of magnitude below that from BM to CC. We neglect these fluxes assuming therefore that continents are formed from back-arc processes rather than from hotspot basalts. However, some authors suggest that the portion of the CC formed from superplumes may be larger than what we consider [56].

The a priori mass fluxes are summarized in Table 2. The uncertainties on these values are difficult to asses but in the parameter inversion discussed later, uncertainties of 50% will be considered. Other mass fluxes are either 0 or are constrained by the masses of CC and D".

5.1.2 Fractionation

In our model, CC is formed from BM. A proxy of the present-day produced continental rocks is andesite. Therefore, for each element i, like U, Pb, Rb, Sr,

$$K^i_{BM\rightarrow CC} = \frac{C^i_{andesite}}{C^i_{MORB\ source}} \tag{8}$$

As we assume that D" is made of partially altered and dehydrated oceanic crust,

$$K^i_{BM\rightarrow D''} = \frac{C^i_{part.\ alt.\ dehyd.\ MORB}}{C^i_{MORB\ source}} \tag{9}$$

Following McCulloch and Gamble [59], the partially altered dehydrated MORBs consists of a mixture of 90% N-MORB plus 10% altered MORB from which 3% fluids are then extracted. RDM should consist primarily of depleted harzburgites in which the element concentrations can be computed from MORB concentrations using Eq. 1 and 2,

$$K^i_{BM\rightarrow RDM} = D_i \frac{C^i_{MORB}}{C^i_{MORB\ source}}. \tag{10}$$

The concentrations used to compute the fractionation coefficients are listed in Table 3.

The fractionation coefficient of He between BM and AT is difficult to constrain because the behavior of He upon melting is not well known. It is thought to be an incompatible element with a solid-melt partition coefficient less than 0.05 [60]. With the simple batch melting equation Eq. 3 and a melt fraction F of 8%, the fractionation coefficient during oceanic crust formation, $K^{He}_{BM\rightarrow OC}$ is $\sim$ 10. There is another contribution to the atmospheric He, namely that produced by CC formation. This contribution is weakly constrained and we assume arbitrarily that the total equivalent fractionation coefficient $K^{He}_{BM\rightarrow AT}$ is 15.

The He in the residual harzburgite reaches eventually the RDM, thus,

$$K^{He}_{BM\rightarrow RDM} = D_{He} K^{He}_{BM\rightarrow OC} \tag{11}$$

Since D_{He} is very uncertain, we choose $K^{He}_{BM\rightarrow RDM}$= 0.01 corresponding to an incompatible behavior. We will see however that a moderately incompatible behavior would also be acceptable. The continental and oceanic crusts are mostly degassed but keep small amounts of He. Therefore, the fractionation coefficients between BM and CC, BM and D" are set to 10^{-3}.

All other fractionation coefficients between silicate reservoirs are equal to 1 as the other mass transfers are not associated with fractionation. Fractionation coefficients between silicate reservoirs and AT are 0, except $K^{He}_{BM\rightarrow AT}$. The fractionation coefficients are summarized in Table 2. Uncertainties of 50% will be considered in the following parameter inversion.

The a priori model includes 22 parameters, namely, the sizes of two reservoirs (RDM and D"), 4 independent fluxes and 16 fractionation coefficients. With this model, the evolutions of 9 isotopes in 5 reservoirs can be computed and compared with observations. Not all 45 present-day possible observations are available. We consider that there are only 17 independent data to constrain our inversion: 4 abundances in the continental crust (those of U, Pb, Rb, and Sr taken from [20]) 12 isotopic ratios (those for $^{3}He/^{4}He$, $^{87}Sr/^{86}Sr$, $^{206}Pb/^{204}Pb$, and $^{207}Pb/^{204}Pb$ for average MORBs, Loihi type and extreme HIMU type basalts, representing BM, RDM and D", respectively), and the CC isotopic Sr ratio.

The uncertainties for the abundances in the CC are about 30%. The standard deviations of the isotopic ratios are estimated according to Zindler and Hart [16]. We assume that these data are independent except for $^{206}Pb/^{204}Pb$ and $^{207}Pb/^{204}Pb$. The isotope ratios of Pb lie on a 1.75 byr isochron and we derive the covariance between the 2 ratios from observations.

6 Results

Having defined all the parameters entering the 5 equations of mass conservation Eq. 6 and the 45 equations of element conservation Eq. 7 we only need to choose the initial concentrations in BM and RDM (the other reservoirs are not present at time $t = 0$) which are assumed primitive [19,61]. The initial isotopic ratios are from Zindler and Hart [16] except for He [61].

To explore the parameter space, a general nonlinear inversion using the least square criterion [62] has been chosen. This method minimizes a misfit function that represents the distance between the predictions and the 17 chosen observations (weighted by their uncertainties), while keeping the 22 parameters listed in Table 2 in the domain defined by their a priori values and uncertainties.

Fig. 4 depicts the minimum misfit as a function of the masses of D" and RDM. The best solutions are obtained for a D" mass of about 220 10^{21} kg (a thickness of 250 km above the CMB) and a RDM mass of 420 10^{21} kg (a thickness of 500 km above D"). The inverted parameters with their uncertainties all lie within their a priori bounds (see Table 4). The number of inverted parameters that can be computed from the resolution matrix of the inversion is about 8 to be compared with a real number of 20 free parameters. In particular, the very small fractionation coefficients are generally poorly constrained. Using

the best parameters, we predict the various isotopic ratios depicted in Fig. 5. Obviously, the ratios for BM, D" and RDM can be associated with those of MORBs, extreme HIMU type and Loihi type basalts.

The predicted concentrations are plotted in Fig. 6. Since only the concentrations in CC have been constrained by the inversion, the others are real predictions. The concentrations in BM which represents more than 80% of the whole mantle can be compared to those of the MORB source given in Table 3. In the D" layer, the composition is very close to that of altered dehydrated oceanic crust (see Table 3) which is another confirmation of the self consistency of our model.

We have assumed that hotspots are tapping a mixture of D" and RDM with a larger D" component for HIMU type hotspots and a larger RDM component for Hawaii. As an example, a mixture of 97% RDM and 3% D" has an isotopic ratio ^{3}He/^{4}He of 5 10^{-5} which is exactly that of Loihi (see Fig. 1) and a U content of 0.006 ppm as calculated by Sims and DePaolo [15]. An equal mixture of RDM and D" has a U content of 0.046 ppm and a He isotopic ratio of 0.9 10^{-5} which are similar to those of Tubuai assuming a melt fraction F of 2%. As the hotspots are fed by the fluxes coming out from RDM and D", $Q_{RDM\rightarrow BM} + Q_{D''\rightarrow BM}$ represents the mass flux of hotspots and the ratio $Q_{D''\rightarrow BM}/(Q_{RDM\rightarrow BM} + Q_{D''\rightarrow BM})$ the percentage of recycled crust in these hotspots. The model predicts that 290 10^{18}kg myr^{-1} of hotspot material containing on average 48 % of recycled crust are delivered to the surface. The ratio of the present day D" mass divided by the total mass of oceanic crust that has entered this reservoir gives the percentage of oceanic crust that has been processed and is now settling at the CMB. It amounts to 20% a value that is acceptable on the basis of convection models [1].

From their U, Pb, Rb and Sr contents, hotspots coming mostly from RDM are equally or more depleted than MORBs although all their isotopic ratios appear primitive. The so-called primitive He ratio of RDM comes mostly from the fact that RDM contains MORB source residuals showing different degrees of degassing and depletion but also that the residence time in RDM is long (2.5 byrs). The hypothesis that He is less incompatible than U [13] is not necessary to predict a RDM reservoir with a high ^{3}He/^{4}He ratio since the He flux from BM to RDM is negligible compared to the He flux from RDM to BM, as soon as $K^{He}_{BM\rightarrow RDM} < 1$ (the mass fluxes are equal but the He concentration is lower in BM than in RDM). Therefore decreasing the He compatibility further or increasing this compatibility up to 1 has barely no effect on the predictions of the model.

7 Discussion and conclusions

Our model does not take into account the time-evolution of the various fluxes with larger CC formation rates and shorter residence times during the Archean [55]. It gives however a reasonable model for the sources of HIMU type and high $^3He/^4He$ Hawaiian type basalts, the former containing a rather large quantity of ancient oceanic crust stagnating near the CMB, the later mostly formed from depleted old harzburgite. In the framework of this model, most of the mantle would be of uniform composition because of a very large mass exchange through the transition zone. The radioactive content of the mantle is predicted to be low as a large part of the radioactive elements (10-30%) are trapped in a layer or in pools [1] of subducted crust. The heat produced by these elements may trigger hotspots at the boundary between a stable D" layer and a depleted RDM.

Such a large quantity of oceanic crust can significantly affect the K budget of the Earth. The K concentration in MORBs being around 900 ppm [57], the K quantity in D" could be comparable to that in CC. The ^{40}Ar stored in D" and produced by ^{40}K could account for $\sim 20\%$ of the total ^{40}Ar of the mantle. This should help to explain the "missing Ar paradox" [63] although it seems necessary to revise the decrease of the quantity of K in the primitive Earth as proposed by Albarède [7] and Davies [64] for a total resolution of the paradox.

In our model we have introduced a layer of segregated oceanic crust and an overlying layer of depleted oceanic lithosphere. It may be, however, that the D" chemical layer is different from or included in the seismologically defined D" layer. The various deep geochemical reservoirs should not be seen as simple shells: they probably have a complex 3-D structure. Only within the framework of complete thermo-chemical convection models will the processes of geochemical evolution be properly treated.

Recently, two models have also tried to explain geochemical data with whole mantle convection [7,65]. According to Kellogg et al. [65], the classical geochemical model with two separated reservoirs can be saved by reducing the size of the primitive reservoir to the bottom 1000 km of the mantle. This latter being intrinsically denser. This model does not explain the origin of D" and may be hard to reconcile with the seismological radial models of the mantle. No such primitive region exists in our model where D" consists of subducted crust. As a consequence, we predict that all hotspots have recycled components. On the contrary Albarède [7] proposes a model in which the lower mantle is younger and more depleted than the upper mantle. In his model, a large mass flux crosses the mantle but fluid dehydration in the transition zone extracts U, Th and K, the radioactive parents of ^4He and ^{40}Ar. This leads to a U concentration in the upper mantle that may be too large for a MORB

source. This depletion effect due to fluid extraction is taken into account in our model where oceanic basalts are altered and dehydrated before reaching the deep mantle, but to a much lower extent.

We do not pretend that our geochemical inversion has constrained the mantle circulation. We have simply shown that starting from a reasonable view of one layer mantle convection, no inconsistencies are found with the geochemical data. The number of parameters (fluxes and fractionation coefficients) is 3 times larger than what can be effectively resolved from data. Better determination of the fractionation coefficients and of their temperature and pressure dependences which may be important would further constrain the geochemical models. We suggest however that the ratio of He and U compatibilities, D_{He}/D_U is not the key parameter to explain MORB-OIB differences.

In essence, we propose a mantle model similar to that of [1] where a significant amount of oceanic crust segregates from the subducting slabs and provides ultimately the source of HIMU basalts. The novelty of our model is to show that such a model is also in agreement with rare gas observations. Whole mantle convection models that are favored by a large number of seismological and geophysical data are thus also supported by geochemical evidence.

Acknowledgements

We would like to thank F. Albarède and Ph. Gillet for constructive discussions, S. Sheppard for improving our English, W. White, G. Davies and P. van Keken for their extensive and fruitful reviews. This work has been supported by CNRS-INSU programs. Some of the computations have been performed thanks to the PSMN computing facilities.

References

[1] U.R Christensen, A.W Hofmann, Segregation of subducted oceanic crust in the convecting mantle, J. Geophys. Res. 99 (1994) 19867–19884.

[2] R.K. O'Nions, E.R. Oxburgh, Heat and helium in the earth, Nature 306 (1983) 429–431.

[3] C.J. Allègre, T. Staudacher, P. Sarda, Rare gas systematics: formation of the atmosphere, evolution and structure of the mantle, Earth Planet. Sci. Lett. 81 (1986) 127–150.

[4] S.P. Grand, R.D. van der Hilst, S. Widiyantoro, Global seismic tomography: a snapshot of convection in the Earth, GSA Today 7 (1997) 1–7.

[5] Y. Ricard, M.A. Richards, C. Lithgow-Bertelloni, Y. LeStunff, A geodynamic model of mantle density heterogeneity, J. Geophys. Res. 98 (1993) 21895–21909.

[6] G.F. Davies, Ocean bathymetry and mantle convection 1. large-scale flow and hotspots, J. Geophys. Res. 93 (1988) 10467–10480.

[7] F. Albarède, Time-dependent models of U-Th-He and K-Ar evolution and the layering of mantle convection, Chem. Geol. 145 (1998) 413–429.

[8] D.L. Anderson, Helium-3 from the mantle: primordial signal or cosmic dust?, Science 261 (1993) 170–176.

[9] M. Moreira, J. Kunz, C.J. Allègre, Rare gas systematics in popping rocks: isotopic and elemental compositions in the upper mantle, Science 279 (1998) 1178–1181.

[10] T. Hanyu, I. Kaneoka, The uniform and low $^3He/^4He$ ratios of HIMU basalts as evidence for their origin as recycled materials, Nature 390 (1997) 273–276.

[11] M.D. Kurz, W.J. Jenkins, S.R. Hart, Helium isotopic systematics of oceanic islands and mantle heterogeneity, Nature 297 (1982) 43–47.

[12] M. Honda, I. McDougall, D.B. Patterson, A. Doulgeris, D.A. Clague, Noble gases in submarine pillow basalt glasses from Loihi and Kilauea, Hawaii: a solar component in the earth, Geochim. Cosmochim. Acta 57 (1993) 859–874.

[13] D. Graham, J. Lupton, F. Albarède, M. Condomines, Extreme temporal homogeneity of Helium isotopes at Piton de la Fournaise, Réunion Island, Nature 347 (1990) 545–548.

[14] A.W. Hofmann, Mantle geochemistry: the message from oceanic volcanism, Nature 385 (1997) 219–229.

[15] K.W. Sims, D.J. DePaolo, Inferences about mantle magma sources from incompatible element concentration ratios in oceanic basalts, Geochim. Cosmochim. Acta 61 (1997) 765–784.

[16] A. Zindler, S. Hart, Chemical geodynamics, Annu. Rev. Earth Planet. Sci. 14 (1986) 493–571.

[17] J.M. Eiler, K.A. Farley, J.W. Valley, A.W. Hofmann, E.M. Stolper, Oxygen isotope constraints on the sources of Hawaiian volcanism, Earth Planet. Sci. Lett. 144 (1996) 453–468.

[18] J. Blichert-Toft, F.A. Frey, F. Albarède, Hf isotope evidence for pelagic sediments in the source of Hawaii, Science 285 (1999) 879–882.

[19] W.F. McDonough, S. Sun, The composition of the Earth, Chem. Geol. 120 (1995) 223–253.

[20] R.L. Rudnick, D.M. Fountain, Nature and composition of the continental crust: a lower crustal perspective, Rev. Geophys. 33 (1995) 267–309.

[21] A.W. Hofmann, W.M. White, Mantle plumes from ancient oceanic crust, Earth Planet. Sci. Lett. 57 (1982) 421–436.

[22] H.N. Pollack, S.J. Hurter, J.R Johnson, Heat flow from the Earth's interior: analysis if the global data set, Rev. Geophys. 31 (1993) 267–280.

[23] N.H. Sleep, Hotspots and plumes: some phenomenology, J. Geophys. Res. 95 (1990) 715–6,736.

[24] H.-P. Bunge, M.A. Richards, J.R. Baumgardener, A sensitivity study of 3-D spherical mantle convection at 10^8 Rayleigh number: effects of depth-dependent viscosity, heating mode and endothermic phase change, J. Geophys. Res. 102 (1997) 11,991–12,022.

[25] B.A. Buffett, H.E. Huppert, J.R. Lister, A.W. Woods, On the thermal evolution of the Earth's core, J. Geophys. Res. 101 (1996) 7989–8006.

[26] S.P. Grand, Tomographic inversion for shear velocity beneath the North American plate, J. Geophys. Res. 92 (1987) 14065–14090.

[27] R.D. van der Hilst, S. Widiyantoro, E.R. Engdahl, Evidence for deep mantle circulation from global tomography, Nature 386 (1997) 578–584.

[28] H. Bijwaard, W. Spakman, E.R. Engdahl, Closing the gap between regional and global travel time tomography, J. Geophys. Res. 103 (1998) 30055–30078.

[29] G. Masters, S. Johnson, G. Laske, H.A. Bolton, A shear-velocity model of the mantle, Phil. Trans. R. Soc. Lond. A 354 (1996) 1385–1411.

[30] P. Machetel, P. Weber, Intermittent layered convection in a model mantle with an endothermic phase change at 670 km, Nature 350 (1991) 55–57.

[31] O.L. Anderson, K. Masuda, D. Guo, Pure silicate perovskite and the PREM lower mantle model: a thermodynamic analysis, Phys. Earth Planet. Inter. 89 (1995) 35–49.

[32] U.R. Christensen, D. Yuen, The interaction of a subducting lithospheric slab with a chemical or phase transition, J. Geophys. Res. 89 (1984) 4389–4402.

[33] P.E. van Keken, C.J. Ballentine, Dynamical models of mantle volatile evolution and the role of phase transitions and temperature-dependent rheology, J. Geophys. Res 104 (1999) 7137–7168.

[34] P. Gillet, I. Daniel, F. Guyot, J. Matas, J.-C. Chervin, A thermodynamic model for $MgSiO_3$-perovskite derived from pressure, temperature and volume dependence of the Raman mode frequencies, Phys. Earth Planet. Int. (1999), in press.

[35] C.G. Farnetani, M.A. Richards, Thermal entrainment and melting in mantle plumes, Earth. Planet. Sc. Lett. 136 (1996) 251–267.

[36] P.E. van Keken, Evolution of starting mantle plumes: a comparison between numerical and laboratory models, Earth Planet. Sci. Lett. 148 (1997) 1–14.

[37] C.G. Farnetani, Excess temperature of mantle plumes: the role of chemical stratification across D", Geophys. Res. Lett. 24 (1997) 1583–1586.

[38] D. McKenzie, Finite deformation during fluid flow, Geophys. J. Roy. Astr. Soc. 58 (1979) 689–715.

[39] M. Gurnis, G.F. Davies, Mixing in numerical models of mantle convection incorporating plate kinematics, J. Geophys. Res. 91 (1986) 6375–6395.

[40] U.R. Christensen, Mixing by time-dependent convection, Earth Planet. Sci. Lett. 95 (1989) 382–394.

[41] S. Ferrachat, Y. Ricard, Regular vs chaotic mixing, Earth Planet. Sci. Lett. 155 (1998) 75–86.

[42] M. Manga, Mixing heterogeneities in the mantle: effect of viscosity differences, Geophys. Res. Lett. 23 (1996) 403–406.

[43] J. Schmaltz, G.A. Houseman, U. Hansen, Mixing properties of three-dimensional stationary convection, Phys. Fluids 7 (1995) 1027–1033.

[44] L.H. Kellogg, D.L. Hunt, Mixing and development of heterogeneities in the mantle: the role of depth-dependent viscosity, J. Geophys. Res. (1999) (submitted)

[45] S.D. King, A. Raefsky, B. Hager, ConMan: vectorizing a finite element code for incompressible two-dimensional convection in the earth's mantle, Phys. Earth Planet. Inter. 59 (1990) 196–208.

[46] P. Lesage, B. Valette, Inferring mean Earth mechanical models from normal modes, mass and inertia: 2. a numerical exploration, to Geophys. J. Int. (1999) (submitted).

[47] R. Widmer, G. Masters, F. Gilbert, Spherical symmetric attenuation within the Earth from normal mode data, Geophys. J. Int. 104 (1991) 541–553.

[48] M.E. Wysession, Continents of the core, Nature 381 (1996) 373–375.

[49] P. Olson, C. Kincaid, Experiments on the interaction of thermal convection and compositional layering at the base of the mantle, J. Geophys. Res. 89 (1991) 425–436.

[50] A.E. Ringwood, T. Irifune, Nature of the 650-km seismic discontinuity: implications for mantle dynamics and differentiation, Nature 331 (1988) 131–136.

[51] S.E. Kesson, J.D. Fitz Gerald, J.M.G. Shelley, Mineral chemistry and density of subducted basaltic crust at lower mantle pressure, Nature 372 (1994) 767–769.

[52] K. Hirose, Y. Fei, Y. Ma, H.-K. Mao, The fate of subducted basaltic crust in the Earth's lower mantle, Nature 397 (1999) 53–56.

[53] G.F. Davies, Mantle plumes, mantle stirring and hotspot chemistry, Earth Planet. Sci. Lett. 99 (1990) 94–109.

[54] G. Schubert, A.P.S. Reymer, Continental volume and freeboard through geological time, Nature 316 (1985) 336–339.

[55] J. Blichert-Toft, F. Albarède, Short-lived chemical heterogeneities in the Archean mantle with implications for mantle convection, Science 263 (1994) 1593–1596.

[56] F. Albarède, The growth of the continental crust, Tectonophysics 296 (1998) 1–14.

[57] A.W. Hofmann, Chemical differentiation of the Earth: the relationship between mantle, continental crust, and oceanic crust, Earth Planet. Sci. Lett. 90 (1988) 297–314.

[58] S.R. Taylor, S.M. McLennan, The continental crust: Its composition and evolution, Blackwell, Cambridge, Mass., 1985.

[59] M.T. McCulloch, J.A. Gamble, Geochemical and geodynamical constraints on subduction zone magmatism, Earth Planet. Sci. Lett. 102 (1991) 358–374.

[60] H. Hiyagon, M. Ozima, Partition of noble gases between olivine and basalt melt, Geochim. Cosmochim. Acta 50 (1986) 2945–2057.

[61] C.L. Harper, S.B. Jacobsen, Noble gases and Earth's accretion, Science 273 (1996) 1814–1818.

[62] A. Tarantola, B. Valette, Generalized nonlinear inverse problems solved using the least square criterion, Rev. Geophys. Space Phys. 20 (1982) 219–232.

[63] C.J. Allègre, A.W. Hofmann, R.K. O'Nions, The Argon constraints on mantle structure, Geophys. Res. Lett. 23 (1996) 3555–3557.

[64] G.F. Davies, Geophysically constrained mantle mass flows and the ^{40}Ar budget: a degassed lower mantle?, Earth Planet. Sci. Lett. 166 (1999) 149–162.

[65] L.H. Kellogg, B.H. Hager, R.D. van der Hilst, Compositional stratification in the deep mantle, Science 283 (1999) 1881–1884.

Fig. 1: $^3He/^4He$ ratios anti-correlate with U contents. MORB data from [57] and [9]. He data of Reunion from [13], of Tubuai from [10], of Tristan and Loihi from [11]. Most of U data from [15].

Fig. 2: Residence times for layers with thickness 1/10 of the box height as a function of depth. The values have been scaled assuming a surface rms velocity of 5 cm yr^{-1} and layer thicknesses of 300 km.

Fig. 3: Geochemical model with 5 reservoirs.

Fig. 4: Minimum misfit as a function of D" and RDM masses. The best solutions are located in the darker region.

Fig. 5: Isotopic ratios of the observed data with their standard deviation ellipsoids (shaded areas) and the predicted values (symbols).

Fig. 6: Abundances of U, Pb, Rb and Sr and ^3He in the various reservoirs for the inverted model and in CC of the a priori model. The a priori standard deviation on CC is 30 %.

Table 1
Masses of the various reservoirs.

Reservoir	D"	RDM	BM	CC	AT
Mass (10^{21}kg)	50-420	80-2700	1000-3800	29	0.052

Table 2
Mass fluxes in 10^{18}kg myr^{-1} and fractionation coefficients.

Parameters	D"	RDM	CC	AT
$Q_{BM\rightarrow}$	180	170	8.5	180
$K^{U}_{BM\rightarrow}$	8.7	0.05	150	-
$K^{Pb}_{BM\rightarrow}$	7.7	0.05	150	-
$K^{Rb}_{BM\rightarrow}$	15	0.009	400	-
$K^{Sr}_{BM\rightarrow}$	6.7	0.3	30	-
$K^{He}_{BM\rightarrow}$	0.001	0.01	0.001	15

Table 3
Concentrations in ppm of MORB source [16], MORB [57] and andesite [58] for Rb, Sr, U and Pb and their solid-melt partition coefficients D_i.

Element	MORB source	MORB	Andesite	D_i	part. alt. dehyd. MORB
Rb	0.096	1.262	42	0.0007	1.48
Sr	13.3	113.2	400	0.04	88.9
U	0.007	0.071	1.25	0.005	0.061
Pb	0.05	0.489	10	0.005	0.385

Table 4
A posteriori parameters and their a posteriori standard deviation. Fluxes are in 10^{18} kg myr^{-1}

Parameters	D"	RDM	CC	AT
$Q_{BM\rightarrow}$	186±53	160±60	10.9±2.5	202±65
$K^{U}_{BM\rightarrow}$	9.5±2.4	0.05±0.02	147±41	-
$K^{Pb}_{BM\rightarrow}$	2.5±0.9	0.05±0.02	137±42	-
$K^{Rb}_{BM\rightarrow}$	16.3±6.7	0.009±0.004	385±170	-
$K^{Sr}_{BM\rightarrow}$	5.7±3.0	0.23±0.13	18.9±5.7	-
$K^{He}_{BM\rightarrow}$	0.0012±0.0005	0.01±0.005	0.001±0.005	16.8±5.4

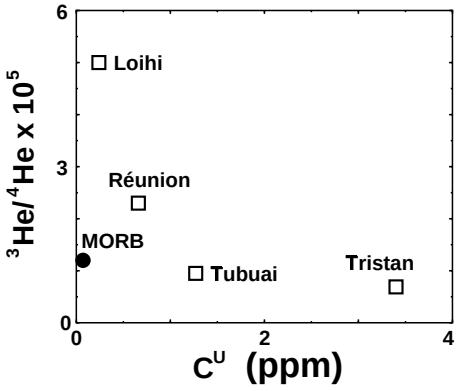
6
3
0
0
2
4
Loihi
Réunion
MORB
Tubuai
Tristan
$^3He/^4He \times 10^5$
C^U (ppm)

Fig. 1.

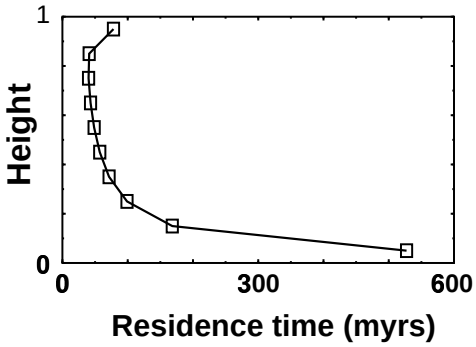
1
0
0
300
600
Height
Residence time (myrs)

Fig. 2.

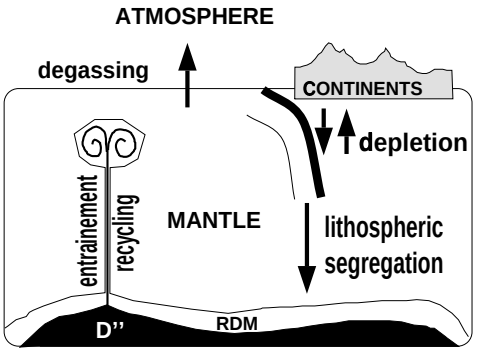
ATMOSPHERE
degassing
CONTINENTS
depletion
entrainement
recycling
MANTLE
lithospheric
segregation
D''
RDM

Fig. 3.

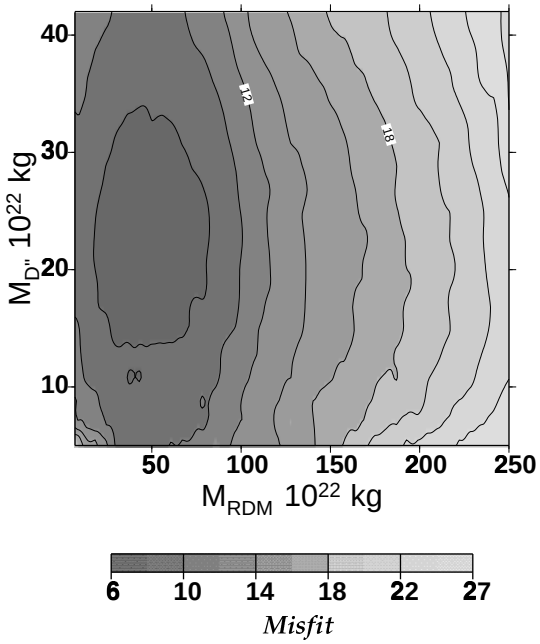
40
30
20
10
$M_{D''}$ 10^{22} kg
50
100
150
200
250
M_{RDM} 10^{22} kg
22
18
6
10
14
18
22
27
Misfit

Fig. 4.

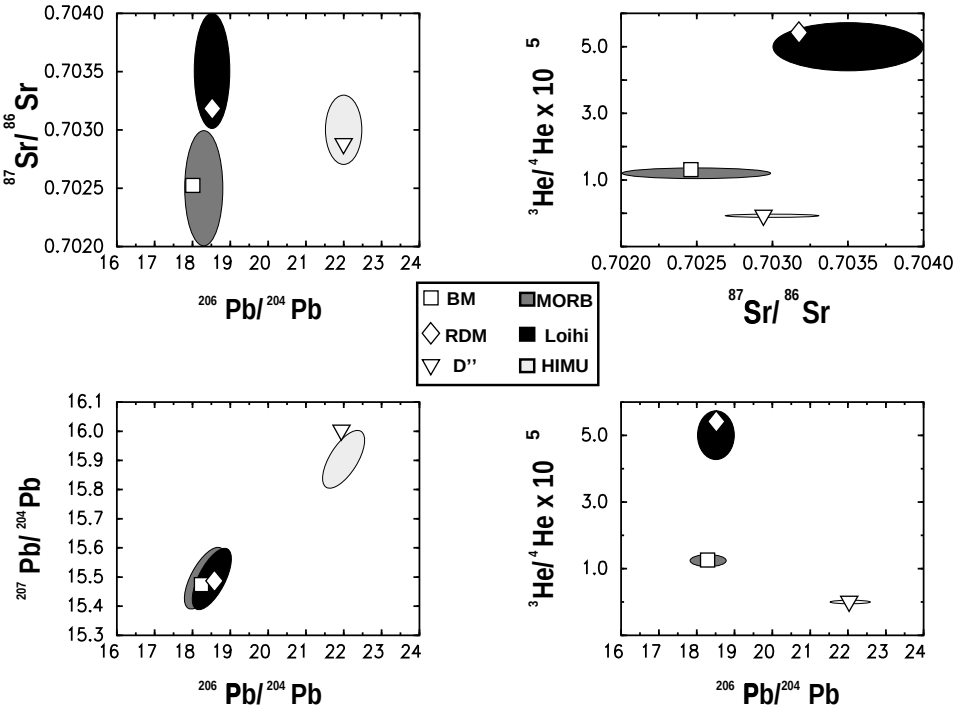
0.7040
0.7035
0.7030
0.7025
0.7020
87Sr/86Sr
16 17 18 19 20 21 22 23 24
206 Pb/204 Pb
BM
MORB
RDM
Loihi
D''
HIMU
5.0
3.0
1.0
3He/4He x 10 5
0.7020 0.7025 0.7030 0.7035 0.7040
87Sr/86Sr
16.1
16.0
15.9
15.8
15.7
15.6
15.5
15.4
15.3
207Pb/204Pb
206 Pb/204 Pb
206 Pb/204 Pb

Fig. 5.

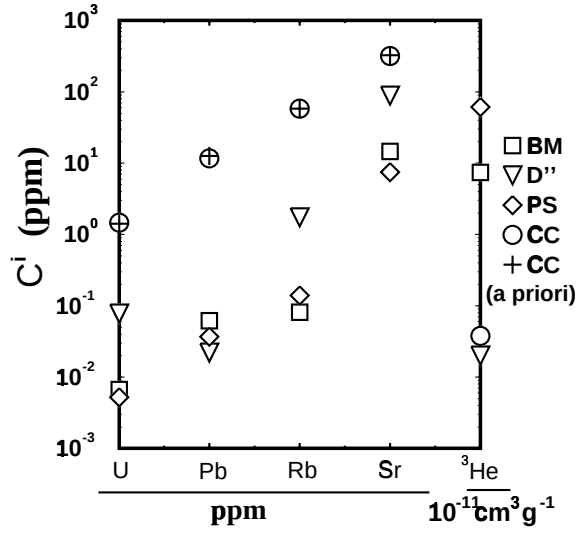
10^3
10^2
10^1
10^0
10^-1
10^-2
10^-3
Ci (ppm)
U
Pb
Rb
Sr
3He
ppm
10-11cm3g-1
BM
D''
PS
CC
CC
(a priori)

Fig. 6.